The α1 and α6 subunit subtypes of the mammalian $GABA_A$ receptor confer distinct channel gating kinetics

Janet L. Fisher

Department of Pharmacology, Physiology and Neuroscience, University of South Carolina School of Medicine, Columbia, SC 29208, USA

The $GABA_A$ receptors show a large degree of structural heterogeneity, with seven different subunit families, and 16 different subtypes in mammalian species. The α family is the largest, with six different subtypes. The α1 and α6 subtypes are among the most diverse within this family and confer distinct pharmacological properties to recombinant and neuronal receptors. To determine whether different single channel and macroscopic kinetic properties were also associated with these subtypes, the α1 or α6 subunit was expressed in mammalian cells along with β3 and γ2L subunits and the kinetic properties examined with outside-out patch recordings. The $\alpha1\beta3\gamma2$L receptors responded to GABA with long-duration openings organized into multi-opening bursts. In contrast, channel openings of the $\alpha6\beta3\gamma2$L receptors were predominately short in duration and occurred as isolated, single openings. The subunit subtype also affected the deactivation rate of the receptor, which was almost 2-fold slower for $\alpha6\beta3\gamma2$L, compared with the $\alpha1\beta3\gamma2$L isoform. Onset of fast desensitization did not differ between the isoforms. To determine the structural domains responsible for these differences in kinetic properties, we constructed six chimeric subunits, combining different regions of the α1 and α6 subunits. The properties of the chimeric subunits indicated that structures within the third transmembrane domain (TM3) and the TM3–TM4 intracellular loop conferred differences in single channel gating kinetics that subsequently affected the deactivation rate and GABA EC_{50}. The effect of agonist concentration on the rise time of the current showed that the extracellular N-terminal domain was largely responsible for binding characteristics, while the transmembrane domains determined the activation rate at saturating GABA concentrations. This suggests that subunit structures outside of the agonist binding and pore-lining domains are responsible for the kinetic differences conferred by the α1 and α6 subtypes. Structural heterogeneity within these transmembrane and intracellular regions can therefore influence the characteristics of the postsynaptic response of $GABA_A$ receptors with different subunit composition.

(Received 1 June 2004; accepted after revision 5 October 2004; first published online 7 October 2004)
Corresponding author J. L. Fisher: Department of Pharmacology, Physiology and Neuroscience, University of South Carolina School of Medicine, Columbia, SC 29208, USA. Email: jfisher@gw.med.sc.edu

The $GABA_A$ receptor (GABAR) mediates the majority of fast inhibitory synaptic transmission in the central nervous system (CNS). Mammalian GABARs are composed of pentameric combinations of $\alpha(1–6)$, $\beta(1–3)$, $\gamma(1–3)$, δ, ε, π or θ subunit subtypes. The pharmacological and physiological properties of GABARs are largely determined by their subunit and subtype composition (Mehta & Ticku, 1999; Korpi *et al.* 2002). Among the six different α subtypes, the α1 and α6 subtypes are the most divergent. The regional expression of α1 and α6 subunit mRNAs in the mammalian brain is different, suggesting distinct physiological roles for these subtypes. The α1 is the most widely expressed of all the α subtypes, and shows a high level of expression in most regions of the brain. Nearly half of all native GABARs in the adult brain are believed to contain an α1 subunit (McKernan & Whiting, 1996). The expression of the α1 subtype mRNA is developmentally regulated, increasing in virtually all brain regions from low levels in embryonic rat to higher levels in the adult (Laurie *et al.* 1992*a*). In contrast, the expression of the α6 subtype is restricted to the granule cells of the cerebellum and cochlea nuclei of the adult (Laurie *et al.* 1992*b*; Varecka *et al.* 1994) where it contributes to both synaptic and extrasynaptic populations (Nusser *et al.* 1998).

 DOI: 10.1113/jphysiol.2003.051839

Substantial effort has focused on describing the pharmacological properties of recombinant GABARs composed of different subunit subtypes and determining the structures responsible for these properties (Korpi *et al.* 2002). However, much less is known about the effect of subtype composition on the single channel properties of these receptors. Among the α subtypes, only the properties of receptors containing $\alpha1$ or $\alpha4$ subunits have been described at the single channel level (Angelotti & Macdonald, 1993; Fisher & Macdonald, 1997; Haas & Macdonald, 1999; Akk *et al.* 2004). Gating characteristics of single channels influence the amplitude, shape and duration of the postsynaptic current. Much of the functional heterogeneity of native GABARs may be due to differences in the subunit composition of the receptors but because most neurones produce a number of different GABAR subunit subtypes, channel characteristics of native receptors cannot be readily assigned to a particular isoform. Previous studies from recombinant receptors have shown that the α subtype influences whole-cell desensitization and deactivation rates (Gingrich *et al.* 1995; Burgard *et al.* 1996; Tia *et al.* 1996*a*, 1996*b*; Lavoie *et al.* 1997; McClellan & Twyman, 1999; Bianchi *et al.* 2002). Additionally, results from transgenic animals suggest that the $\alpha1$ subunit is necessary for a developmental shift in decay rate observed in many brain regions, supporting the idea that changes in the relative levels of α subtypes alter the kinetic properties of the receptors (Vicini *et al.* 2001; Goldstein *et al.* 2002; Koksma *et al.* 2003). Pathological conditions such as anxiety and epilepsy are also associated with changes both in α subtype expression and IPSC decay kinetics (Smith *et al.* 1998; Hsu *et al.* 2003; Cagetti *et al.* 2003).

The $\alpha1$ and $\alpha6$ subtypes share the least structural homology of the α family members (59% amino acid identity) (Lüddens *et al.* 1990; Tyndale *et al.* 1995). Which of the structural differences among the subtypes are functionally important in determining the unique channel characteristics associated with each receptor isoform? Determining the structures that regulate these properties will not only increase our understanding of the physical mechanisms that underlie channel function, but will also suggest potential targets for the development of drugs selective for these receptor isoforms. Most of the mutational analysis of GABAR subunits has examined agonist binding and transduction sites for GABA and allosteric modulators (Mehta & Ticku, 1999; Korpi *et al.* 2002), and little is known about the non-conserved sites that contribute to the unique characteristics associated with different subunits and subtypes.

The differences in the amino acid sequences between $\alpha1$ and $\alpha6$ subtypes occur primarily in the large extracellular N-terminal domain and in the intracellular loop between the third and fourth transmembrane domains (TMs), while the TMs themselves and the TM2–TM3 extracellular domain are highly conserved (83% amino acid identity). To determine the structural domains responsible for the different kinetic properties associated with the $\alpha1$ and $\alpha6$ subtypes, chimeric constructs of the rat $\alpha1$ and $\alpha6$ subunits were created with three different splice sites (Fig. 1). Plasmids containing the wild-type subunits or chimeric constructs were transiently transfected along with $\beta3$ and $\gamma2$L subunits into a human embryonic kidney cell line (HEK-293T) and the receptor properties were measured through whole-cell, single channel and rapid application recordings.

Methods

Construction of chimeric subunits

Full-length cDNAs for rat $\alpha1$, $\alpha6$, $\beta3$ and $\gamma2$L GABAR subunits were obtained in the mammalian expression vectors pCMVneo (Robert Macdonald, Vanderbilt University). The A-site chimeras have already been characterized at the whole-cell level and the methods for construction of the chimera published (Fisher *et al.* 1997). To produce the other chimeric subunits, $\alpha1$ and $\alpha6$ cDNAs were subcloned into the pcDNA1.1/Amp plasmid (Invitrogen). Chimeras at splice sites B and C (Fig. 1) were created by taking advantage of unique restriction sites at these locations in the $\alpha1$ and $\alpha6$ subunits. In each case a single mutation was required in one subunit to either create or remove a restriction site. Mutations were made in the GABAR subunit cDNA using a commercial kit (QuikChange, Stratagene) and verified with sequencing of both strands. These mutations were silent, changing

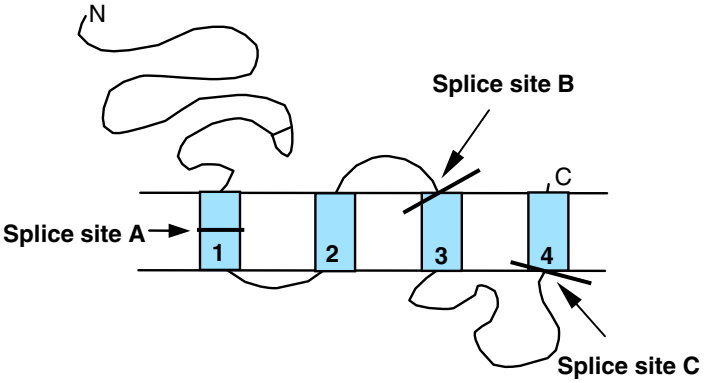

Figure 1. Locations of the splice sites for generation of the chimeric subunits
Schematic representation of a GABAR subunit. The GABAR subunit structure includes four transmembrane domains (TM1–TM4), a large N-terminal extracellular domain, and a large intracellular domain between TM3 and TM4. The splice sites for the chimeric subunits were located within TM1 (site A), on the extracellular side of TM3 (site B), and on the intracellular side of TM4 (site C) as shown by the arrows.

the nucleotide sequence but not the amino acid sequence. Once these restriction sites were in place, the plasmids were cut to release the section of the subunit from the splice site through a portion of the vector. The fragments were then gel-purified, swapped and re-ligated. Creation of the expected chimera was verified by sequencing. For the B-site chimera, a *Nco* I site was utilized at the start of TM3. This was a unique site in the α6 subunit. An additional *Nco* I site was removed from the α1 subunit with a CCT to CCC mutation, encoding a proline in both cases. For the C-site chimera, a unique *Bsp*106I site at the start of the TM4 was created in the α6 subunit with an ATA to ATC mutation, encoding an isoleucine residue in both cases. To produce this same restriction site in the α1, GAC was mutated to GAT, both encoding an aspartate residue.

Transfection of HEK-293T cells

Wild-type or chimeric α subunits were transiently transfected along with β3 and γ2L subunits into the human embryonic cell line HEK-293T (Genhunter, Nashville, TN, USA). The β3 and γ2L subtypes were selected for co-expression because they are found at high levels in most regions of the brain and may therefore potentially represent native isoforms. In addition, the kinetic properties of the $\alpha1\beta3\gamma2$L isoform have been well described, and these previous reports provide a useful background for comparison (Fisher & Macdonald, 1997; Haas & Macdonald, 1999).

For selection of transfected cells, the plasmid pHook-1 (Invitrogen, San Diego, CA, USA) containing cDNA encoding the surface antibody sFv was also transfected into the cells. Cells were maintained in Dulbecco's modified Eagle medium (DMEM) plus 10% fetal bovine serum, 100 IU ml^{-1} penicillin and 100 μg ml^{-1} streptomycin. Cells were passaged by a 5 min incubation with 0.05% trypsin−0.02% EDTA solution in phosphate-buffered saline (10 mM Na_2HPO_4, 150 mM NaCl, pH = 7.3).

The cells were transfected using a modified calcium phosphate method (Angelotti *et al.* 1993). Plasmids encoding GABAR subtype cDNAs were added to the cells in 1 : 1 ratios of 2 μg each plus 1 μg of the plasmid encoding sFv. Following a 4–6 h. incubation at 3% CO_2, the cells were treated with a 15% glycerol solution in BBS buffer (50 mM Bes (*N,N*-bis[2-hydroxyethyl]-2-aminoethanesulphonic acid), 280 mM NaCl, 1.5 mM Na_2HPO_4) for 30 s. The selection procedure for sFv antibody expression was performed 20–28 h later as described in Greenfield *et al.* (1997). Briefly, the cells were passaged and mixed with 3 μl of magnetic beads coated with hapten (approximately 4.5×10^5 beads) (Chesnut *et al.* 1996). Following 30–60 min of incubation to allow the beads to bind to positively transfected cells, the beads and bead-coated cells were isolated using a magnetic stand. The selected cells were resuspended into DMEM, plated onto poly-lysine-treated glass coverslips coated with collagen and used for recording 18–28 h later.

Electrophysiological recording solutions and techniques

For all recordings the external solution consisted of (mM): 142 NaCl, 8.1 KCl, 6 $MgCl_2$, 1 $CaCl_2$, 10 glucose and 10 Hepes (4-(2-hydroxyethyl)-1-piperazine-ethanesulphonic acid) with pH = 7.4 and osmolarity adjusted to 295–305 mosmol l^{-1}. Recording electrodes were filled with an internal solution of (mM): 153 KCl, 1 $MgCl_2$, 5 K-EGTA (ethylene glycol-bis (β-aminoethyl ether *N,N,N′N′*-tetraacetate), 2 MgATP and 10 Hepes with pH = 7.4 and osmolarity adjusted to 295–305 mosmol l^{-1}. These solutions provided a chloride equilibrium potential near 0 mV. For single channel recordings the electrodes were coated with polystyrene Q-dope (GC Electronics). GABA was diluted into external solution from freshly made or frozen stocks in water. Patch pipettes were pulled from borosilicate glass with an internal filament (World Precision Instruments, Sarasota, FL, USA) on a two-stage puller (Narishige, Japan) to a resistance of 5–10 MΩ. For whole-cell recordings and single channel recordings GABA was applied to cells or excised outside out patches using a stepper solution exchanger with a complete exchange time of < 50 ms (open tip, SF-77B, Warner Instruments, Hamden, CT, USA). For macropatch rapid-application recordings the 3-barrel square glass was pulled to a final size near 200 μm. The 10–90% rise times of the junction potential at the open tip were consistently faster than 400 μs and were tested after each patch recording using a diluted external solution. There was a continuous flow of external solution through the chamber. Currents were recorded with an Axon 200B (Foster City, CA, USA) patch clamp amplifier and stored on hard drive for off-line analysis. All experiments were performed at room temperature (near 25°C).

Analysis of currents

Whole-cell currents were analysed using the programs Clampfit (pCLAMP8 suite, Axon Instruments, Foster City, CA, USA) and Prism (Graphpad, San Diego, CA, USA). Concentration–response data were fitted with a four-parameter logistic equation:

$$\text{Current} = \frac{\text{maximum current}}{1 + 10^{(\log EC_{50} - \log[GABA])n)}}$$

where n represents the Hill number. Fits were made to normalized data with current expressed as a percentage of the maximum response to GABA for each cell.

Macropatch currents were digitized at 10 kHz and analysed with the pCLAMP8 suite of programs (Axon Instruments). The desensitization or deactivation rate was determined by fitting the decay current with the Levenberg-Marquardt least squares method with one or two exponential functions, as determined by a significant improvement of the fit with additional components (F test of the sum of squared residuals). Weighted mean decay times were calculated by multiplying each time constant by its relative area.

Single channel currents were recorded on digital tape for offline analysis. Recordings were digitized at 20 kHz and filtered at 2 kHz. Open and closed intervals were detected with a 50% threshold method, with a transition recorded every time the current passed a threshold set at one-half of the amplitude of the main conductance level (Fetchan, pCLAMP8). Sub-conductance openings were rarely observed ($< 0.1\%$ of openings), and were not included in the analysis. Stability plots of open probability showed no time-dependent changes in channel activity. Analysis of the event dwell-times was performed with the Interval 5 program (Dr Barry Pallotta, University of North Carolina-Chapel Hill) using the maximum likelihood fitting method. The number of components required to fit the interval histograms was increased until an additional component did not significantly improve the fit (Horn, 1987). Confidence limits for the components of each fit were calculated by the method of m-unit likelihood intervals (Colquhoun & Sigworth, 1995). To define bursts the briefest one or two closed components were considered intraburst closures. The critical gap was calculated from the closed interval histogram for each patch using a method that equalized the proportions of misclassified events (Colquhoun & Sakmann, 1985).

Tukey-Kramer multiple comparisons tests were performed using the Instat program (Graphpad) with a significance level of $P < 0.05$. The logs of the GABA EC_{50} measurements were used for statistical comparison.

Results

The α1 and α6 subtypes confer different single channel kinetic properties

The α1 and α6 subtypes of the GABAR show distinct patterns of distribution throughout the brain and through development. These subtypes confer very different pharmacological properties to recombinant and native receptors. While some studies have examined the kinetic properties associated with these subunits at the whole-cell level, the single channel characteristics of receptors containing the α6 subtype have not been described. Channel gating properties influence the amplitude and duration of the postsynaptic response to GABA. Therefore, differences in these properties due to varying subunit composition could alter the effectiveness of GABAergic neurotransmission.

To compare the kinetic properties of $\alpha1\beta3\gamma2$L and $\alpha6\beta3\gamma2$L receptor channels, outside-out patches were exposed to submaximal ($\sim EC_{20-30}$) GABA concentrations for each isoform (10 μM for $\alpha1\beta3\gamma2$L and 1 μM for $\alpha6\beta3\gamma2$L). The durations of channel openings and closures were obtained from steady-state recordings (5–10 min). The $\alpha1\beta3\gamma2$L receptors were characterized by relatively long-duration openings, which occurred in a pattern of bursts (Fig. 2) (Fisher & Macdonald, 1997). In contrast, the $\alpha6\beta3\gamma2$L channel openings were relatively brief in duration, and tended to occur as isolated single openings rather than in bursts.

The open duration histograms for the $\alpha1$ subtype-containing channels were best fitted with the sum of three exponential distributions, and all three of the open states made a substantial contribution to the total area (Fig. 2*B*, Table 1, 1226–5377 open intervals per patch). However, the $\alpha6$ subtype-containing receptors only rarely exhibited a third, long-duration open state. Although open interval histograms from some (3 of 7) of the $\alpha6\beta3\gamma2$L patches were best fitted with three distributions, the longest open state contributed less than 1% of the area in all cases (Fig. 2*B*, Table 1, 2454–5278 open intervals per patch). Therefore, the mean open time of the $\alpha6\beta3\gamma2$L receptors was significantly briefer than the $\alpha1\beta3\gamma2$L receptors (Table 1). The relative areas of all the open states were significantly different between the receptor isoforms (Table 1). The time constant (τ) of the second longest open state was also significantly shorter for the $\alpha6\beta3\gamma2$L receptor. This may reflect difficulty in accurately fitting components with low relative area, or may indicate a true difference in the stability of this open conformation. When examining only the histograms fitted best with three components, the 95% confidence limits for the time constant of the second open state showed a larger range (0.555–7.964 ms, mean of 1.15 ms) than the fits to the other states, which were typically less than 1.5 times the mean. For example, the 95% confidence limits for the longest open state in these histograms had a range of 4.05–6.68 ms (mean of 5.53 ms). When all open histograms from $\alpha6$ subunit-containing receptors were fitted with only two exponential distributions, the average time constant for the longer open state was not significantly different from the 2nd longest open state of the $\alpha1\beta3\gamma2$L channels.

The closed interval histograms for the $\alpha1\beta3\gamma2$L channels were best fitted with the sum of five exponential distributions (Fig. 2*B*). Because the durations and relative contributions of longer closed states are subject to greater error with multi-channel patches, only the briefer closures and burst properties were examined in detail.

The two briefest components, generally considered intraburst closures, made a large contribution ($65.3 \pm 3.9\%$, $n = 6$) to the total area. The histograms for the $\alpha6\beta3\gamma2$L isoform were fitted with four or five components, and often lacked one of the two briefest components compared with $\alpha1\beta3\gamma2$L (Fig. 2*B*). In contrast to receptors containing the $\alpha1$ subtype, the shorter closed components ($\tau < 10$ ms) made a minor contribution to the total area, averaging $19.8 \pm 5.2\%$ ($n = 7$, $P < 0.001$ compared with $\alpha1\beta3\gamma2$L), consistent with the isolated appearance of these channel openings. As with the longest open state, the rare relative occurrence of these brief closures led to difficulty in discriminating these components and accurately fitting their time constants.

To examine the burst properties of these isoforms, a critical gap (τ_{crit}) representing the termination of bursts was defined between the brief closed components. For the $\alpha1\beta3\gamma2$L receptor and for $\alpha6\beta3\gamma2$L patches fitted with five exponential distributions, the two shortest components were assigned as intraburst closures. For histograms from $\alpha6\beta3\gamma2$L receptors fitted with four components, only the briefest was considered intraburst since the next shortest component had a τ greater than 10 ms, and was therefore more comparable to the third-longest closed component of the $\alpha1\beta3\gamma2$L receptor. Using these techniques, the τ_{crit} was not significantly different between the isoforms, with an average of 1.96 ± 0.17 ms for $\alpha1\beta3\gamma2$L and 2.10 ± 0.28 ms for $\alpha6\beta3\gamma2$L ($P > 0.05$). Distributions of burst durations were fitted with the sum of three exponential distributions, and distributions of openings/burst were fitted with the sum of two to three geometric functions. The $\alpha1\beta3\gamma2$L receptors showed significantly longer average burst durations (6.91 ± 1.05 ms, $n = 6$) compared with the $\alpha6\beta3\gamma2$L receptors (0.96 ± 0.19 ms, $n = 7$). The average number of openings per burst was also higher for $\alpha1\beta3\gamma2$L receptors (2.49 ± 0.25 openings, $n = 6$) compared with $\alpha6\beta3\gamma2$L (1.41 ± 0.09 openings, $n = 7$).

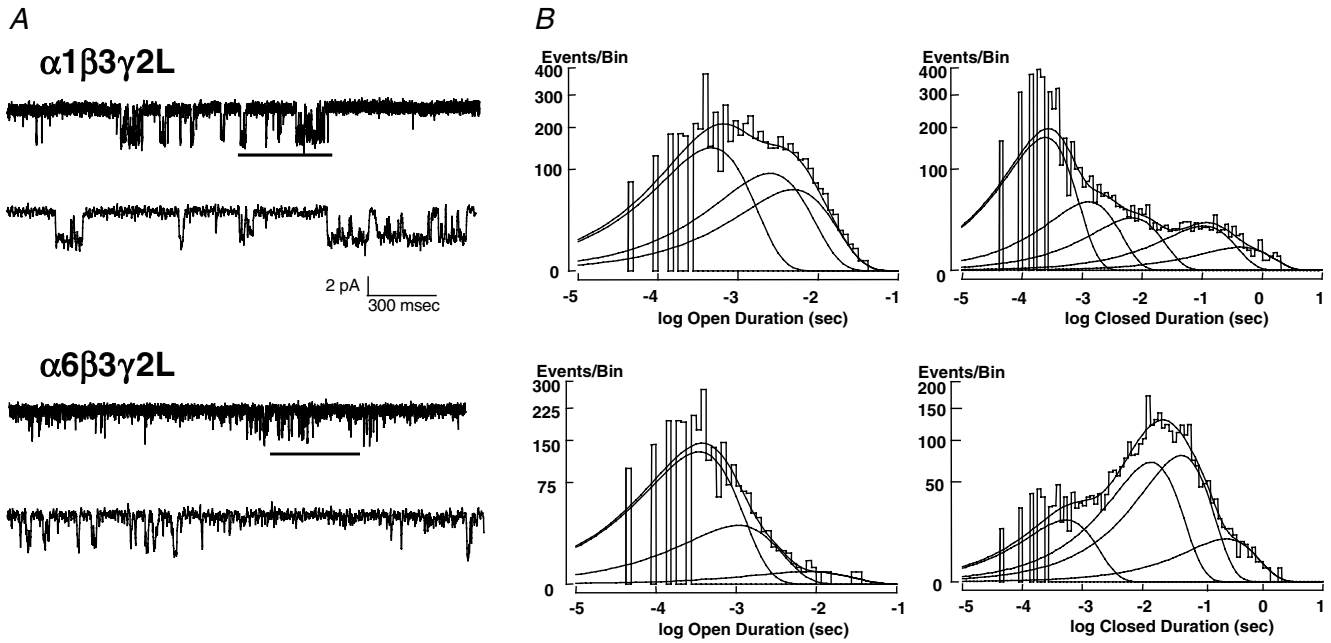

Figure 2. Single channel characteristics of receptors containing α1 or α6 subunit subtypes
A, single channel GABAR currents were obtained from outside-out patches. Upper traces are continuous 10 s recordings from patches in response to 1 μM ($\alpha6\beta3\gamma2$L) or 10 μM GABA ($\alpha1\beta3\gamma2$L). The lower trace shows a 2 s segment extracted from the upper trace, as indicated by the bar. Patches were held at −100 mV. In this and all subsequent figures, channel openings are downward. For display the data were sampled at 1 ms per point and filtered at 100 Hz. *B*, duration histograms of open and closed intervals from individual patches were fitted with the sum of three to five exponential functions. For $\alpha1\beta3\gamma2$L, the individual components for the open interval histogram shown had time constants (and relative areas) of 0.54 ms (0.485), 2.88 ms (0.304), and 5.64 ms (0.211) with 5377 intervals and a mean open time of 2.33 ms. The closed interval histogram was fitted with five components with time constants (and relative areas) of 0.28 ms (0.639), 1.48 ms (0.170), 7.8 ms (0.10), 123.3 ms (0.072) and 507.7 ms (0.019). For $\alpha6\beta3\gamma2$L the open interval histogram shown was fitted with three components with time constants (and relative areas) of 0.40 ms (0.829), 1.21 ms (0.164) and 8.96 ms (0.007) with 2454 intervals and a mean open time of 0.59 ms. The closed interval histogram was fitted with four components with time constants (and relative areas) of 0.61 ms (0.107), 16.05 ms (0.396), 50.7 ms (0.446) and 283.0 ms (0.051).

Table 1. Open interval properties

	τ1 (ms) (% area)	τ2 (ms) (% area)	τ3 (ms) (% area)	Mean open time (ms)
$\alpha1\beta3\gamma2$L ($n = 6$)	0.53 ± 0.03 (50.5 ± 2.8%)†††	3.30 ± 0.44† (32.9 ± 2.5%)†††	6.35 ± 0.45 (16.6 ± 2.1%)†††	2.41 ± 0.27†††
$\alpha6\beta3\gamma2$L ($n = 7$)	0.36 ± 0.03 (91.3 ± 2.2%)***	1.48 ± 0.29* (8.0 ± 2.1%)***	5.53 ± 1.8 (0.7 ± 0.5%)***	0.46 ± 0.05***
$\alpha1/\alpha6$-A ($n = 6$)	0.37 ± 0.03 (91.9 ± 1.3%)***	1.42 ± 0.15* (7.8 ± 1.3%)**	5.22 ± 3.0 (0.3 ± 0.2%)***	0.47 ± 0.04***
$\alpha1/\alpha6$-B ($n = 5$)	0.34 ± 0.05 (93.0 ± 2.5%)***	1.37 ± 0.25* (6.8 ± 2.5%)**	6.17 ± 1.8 (0.2 ± 0.1%)***	0.42 ± 0.08***
$\alpha1/\alpha6$-C ($n = 6$)	0.47 ± 0.06 (44.9 ± 4.1%)†††	2.88 ± 0.38† (35.7 ± 2.1%)†††	5.86 ± 0.30 (19.4 ± 2.5%)†††	2.42 ± 0.30†††
$\alpha6/\alpha1$-A ($n = 5$)	0.36 ± 0.06 (36.5 ± 5.0%)†††	2.27 ± 0.16 (46.6 ± 7.9%)†††	5.84 ± 0.99 (16.9 ± 5.1%)†††	2.25 ± 0.36†††
$\alpha6/\alpha1$-B ($n = 5$)	0.52 ± 0.05 (50.1 ± 8.3%)†††	2.65 ± 0.64 (37.6 ± 8.8%)†††	6.04 ± 2.0 (12.3 ± 1.9%)††	1.82 ± 0.26†††
$\alpha6/\alpha1$-C ($n = 6$)	0.39 ± 0.02 (95.2 ± 0.8%)***	1.57 ± 0.17* (4.3 ± 0.9%)***	5.23 ± 0.82 (0.5 ± 0.3%)***	0.45 ± 0.27***

Significantly different from $\alpha1\beta3\gamma2$L: $^{*}P < 0.05$, $^{**}P < 0.01$, $^{***}P < 0.001$. Significantly different from $\alpha6\beta3\gamma2$L: †$P < 0.05$, ††$P < 0.01$, †††$P < 0.001$.

At the submaximal GABA concentration used here, the $\alpha6\beta3\gamma2$L receptors rarely enter long open states. For the $\alpha1\beta3\gamma2$L isoform, higher GABA concentrations lead to a greater proportion of longer open states (Fisher & Macdonald, 1997). The longer open states are also associated with longer bursts, both in mean duration and in the number of openings per burst (Twyman *et al.* 1990). Therefore, higher GABA concentrations also lead to a greater contribution from the briefer closed states, which are best modelled as terminal states connected to each of the open states (Twyman *et al.* 1990; Haas & Macdonald, 1999). If the burst structure for the $\alpha6\beta3\gamma2$L receptor channels is similar to that for the $\alpha1\beta3\gamma2$L isoform, higher GABA concentrations might lead to an increased contribution from longer open states, leading to greater openings per bursts and more brief closures. This could clarify the time constants for these components of the closed and open interval histograms.

Design of $\alpha1/\alpha6$ chimeric subunits

These results show that the $\alpha1$ and $\alpha6$ subtypes confer distinct channel gating kinetics to recombinant receptors. To examine the structural differences between the subunits responsible for these characteristics, chimeric subunits of the $\alpha1$ and $\alpha6$ subunits were designed to isolate the contributions of the transmembrane domains. The chimeric subunits contained the structure of one of the α subtypes up to the splice site, with the remainder of the subunit structure from the other subtype. The splice sites were located within TM1 (site A), at the N-terminal side of TM3 (site B) and at the N-terminal side of the TM4 (site C) (Fig. 1). The region of the subunit between splice sites A and B included the TM2 and a short extracellular domain between TM2 and TM3. The region between splice sites B and C spanned TM3 and the large intracellular loop between TM3 and TM4. For the C-site chimeras only the TM4 and the short extracellular C-terminal domain was contributed from the other subtype.

Single channel properties of receptors containing chimeric subunits

Steady-state recordings were made from outside-out patches at a holding potential of −100 mV in response to continuous application of an $EC_{20–30}$ GABA concentration for each isoform. The channel openings produced by the $\alpha6/\alpha1$-A$\beta3\gamma2$L receptor in response to 0.3 μM GABA were similar to the $\alpha1\beta3\gamma2$L isoform, occurring in a series of bursts, with a significant contribution from long-duration openings (Fig. 3). Fits of open interval histograms showed that these channels produced three open states, with average durations and relative contributions comparable to those seen with the $\alpha1\beta3\gamma2$L isoform (Table 1). The burst characteristics were also similar to the $\alpha1$ subtype-containing receptors (Fig. 3*B*). None of these properties were significantly different from the $\alpha1\beta3\gamma2$L receptor ($P > 0.1$). In contrast, the $\alpha1/\alpha6$-A chimeric subunit, which contained the N-terminal domain of the $\alpha1$ subtype, produced channel openings that were predominantly brief in duration (Fig. 3). The open

state and burst characteristics were similar to receptors containing the wild-type α6 subunit (Table 1, Fig. 3*B*) and none of the kinetic properties were significantly different from $\alpha6\beta3\gamma2$L ($P > 0.1$). The large extracellular domain is responsible for much of the structural heterogeneity between the α subtypes; however, it does not appear to make a significant contribution to the differences in single channel kinetics. Therefore, structural differences within the agonist binding sites are not likely to be responsible for the differences between the α1 and α6 subunits in channel gating characteristics.

The role of the TM2 and its flanking domains was examined with the B-site chimeras, which exchanged the N-terminal domain of the subunits through the start of TM3. Like the A-site chimeric subunits, the $\alpha6/\alpha1$-B$\beta3\gamma2$L receptors were similar to $\alpha1\beta3\gamma2$L receptors in their channel properties, with the longest of three open states making a significant contribution to the area of the open interval histogram (Fig. 3, Table 1). The burst characteristics were also indistinguishable from receptors containing the α1 subtype (Fig. 3*B*). None of these kinetic properties were significantly different from the $\alpha1\beta3\gamma2$L receptor ($P > 0.1$). Again, as with the A-site chimera, the $\alpha1/\alpha6$-B chimeric subunit conferred single channel characteristics similar to the $\alpha6\beta3\gamma2$L receptor, with predominantly brief-duration, isolated openings

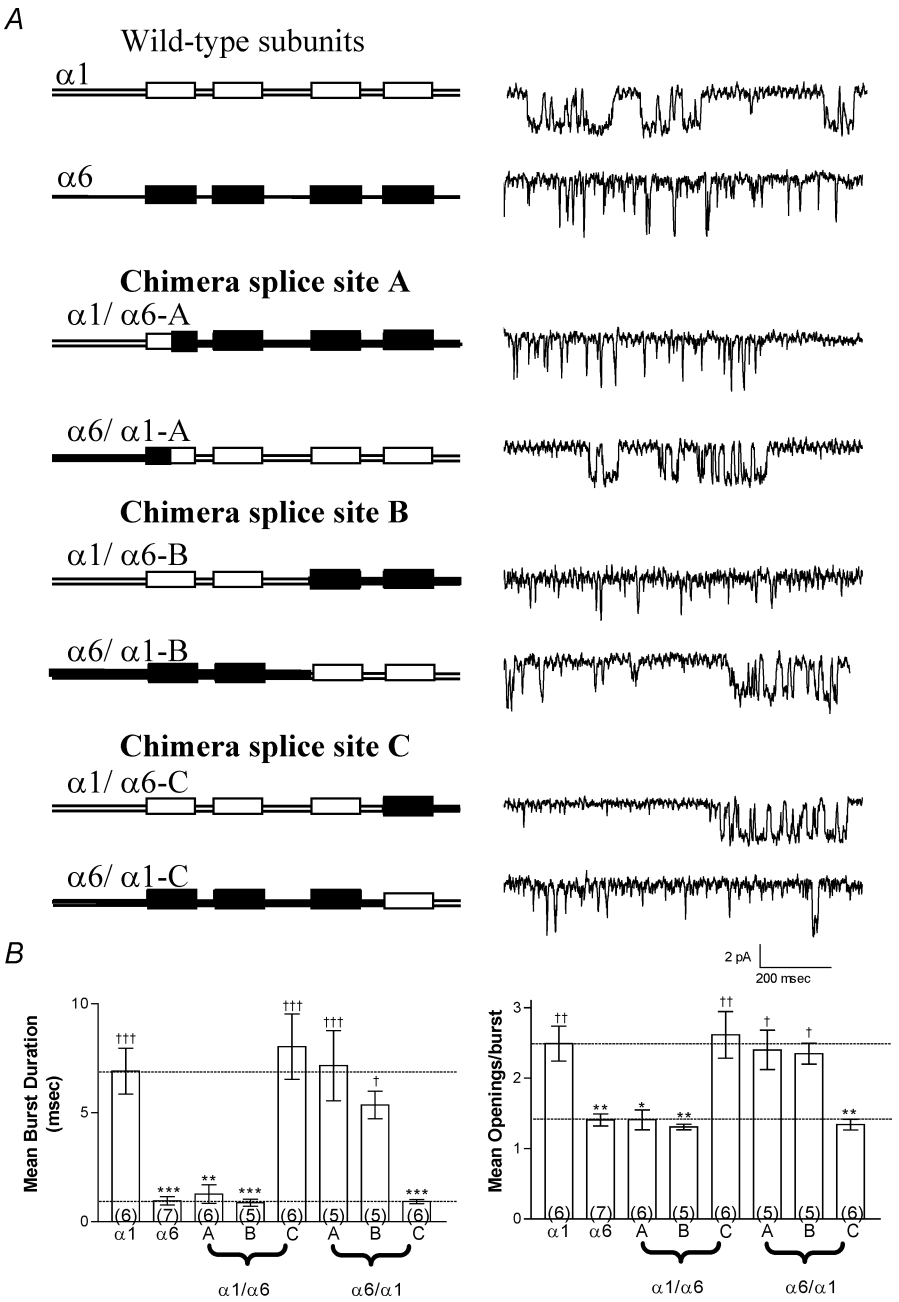

Figure 3. Single channel and burst properties of receptors containing chimeric subunits
A, traces shown are continuous 1 s recordings from outside-out patches in response to steady-state applications of 0.3 μM ($\alpha6/\alpha1$-A, $\alpha6/\alpha1$-B), 1 μM ($\alpha6$, $\alpha6/\alpha1$-C), 10 μM ($\alpha1$, $\alpha1/\alpha6$-C) or 30 μM GABA ($\alpha1/\alpha6$-A, $\alpha1/\alpha6$-B). Patches were voltage clamped at -100 mV. For display the data were sampled at 500 μs per point and filtered at 100 Hz. Schematics of the chimeric constructs are shown to the left, with boxes indicating the transmembrane domains. *B*, mean burst durations were calculated by weighting the time constants from the fit of the histograms by their relative areas. Histograms were typically fitted with three components. The average number of openings per burst were calculated by a weighted mean of the fit of the openings/burst distributions, which were typically fitted with the sum of two to three geometric components. Bars represent means ± S.E.M. and the numbers in parentheses indicate the number of patches. Dotted lines represent the mean of the wild-type receptors. $^*P < 0.05$, $^{**}P < 0.01$ and $^{***}P < 0.001$ indicate a significant difference from $\alpha1\beta3\gamma2$L. $\dagger P < 0.05$, $\dagger\dagger P < 0.01$ and $\dagger\dagger\dagger P < 0.001$ indicate a significant difference from $\alpha6\beta3\gamma2$L.

(Fig. 3, Table 1). The open state and burst properties were not significantly different from the $\alpha6\beta3\gamma2$L isoform.

The C-site chimeras examined the contribution from TM4 to the single channel characteristics. Receptors containing the $\alpha6/\alpha1$-C chimeric subunit had single channel properties similar to those with the $\alpha6$ subunit, with isolated, brief-duration openings (Fig. 3, Table 1). The open state and burst properties were not significantly different from the $\alpha6\beta3\gamma2$L receptor ($P > 0.1$). Channel openings from $\alpha1/\alpha6$-C$\beta3\gamma2$L receptors were similar to those containing the $\alpha1$ subtype, with long-duration openings occurring in a pattern of bursts (Fig. 3, Table 1). None of the single channel kinetic properties differed significantly from the $\alpha1\beta3\gamma2$L receptor ($P > 0.1$).

These findings suggest that the region of the subunit that includes TM3 and the TM3–TM4 intracellular domain contains the structural differences responsible for the unique kinetic properties associated with the $\alpha1$ and $\alpha6$ subtypes. The N-terminal extracellular domain and the 1st, 2nd and 4th transmembrane domains do not appear to contribute to the differences in open state or burst properties between the $\alpha1$ and $\alpha6$ subtypes. Additional chimeric constructs exchanging only the TM3 and TM3–TM4 domains would be necessary to confirm that interactions with other regions do not contribute to these single channel properties.

GABA sensitivity of receptors containing $\alpha1/\alpha6$ chimeric subunits

Consistent with previous reports (Ducic *et al.* 1995; Saxena & Macdonald, 1996; Fisher *et al.* 1997), the $\alpha1\beta3\gamma2$L and $\alpha6\beta3\gamma2$L isoforms differed in their GABA sensitivity. GABA was applied for 5 s to cells voltage-clamped at −50 mV in the whole-cell recording configuration. The GABA EC_{50} was about 10 times higher for receptors containing the $\alpha1$ subtype compared with those with the $\alpha6$ subtype (Fig. 4). The average GABA EC_{50} for the $\alpha1\beta3\gamma2$L receptors was $18.5 \pm 1.7\ \mu$M ($n = 5$), while that of the $\alpha6\beta3\gamma2$L receptors was $1.8 \pm 0.22\ \mu$M ($n = 7$). To examine the structural differences between the subunits that contribute to this pharmacological difference, we examined the GABA sensitivity of receptors containing each of the chimeric subunits.

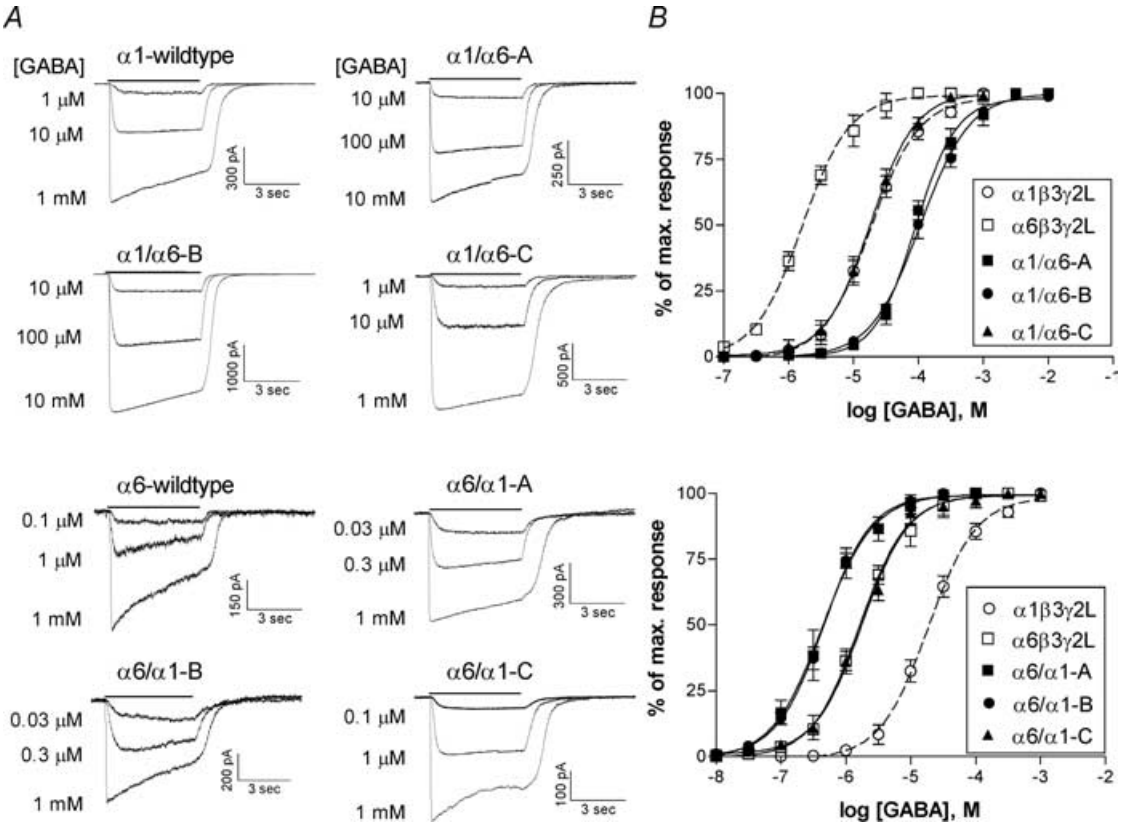

Figure 4. GABA sensitivity of receptors containing wild-type and chimeric subunits
A, representative whole-cell traces from transfected HEK-293T cells. The peak current in response to varying concentrations of GABA was measured. GABA was applied for 5 s, as indicated by the bar, to cells voltage clamped at −50 mV. The same time scale applies to all traces. *B*, concentration–response relationships were constructed by normalizing the peak response to each concentration of GABA as a percentage of the maximum current response for each cell. Points shown are the means ± S.E.M. ($n = 4$–7 cells). Averaged data were fitted with a four-parameter logistic equation represented by the dashed (wild-type) or continuous (chimeras) line.

The measured GABA EC_{50} is influenced by downstream signal transduction events as well as by the binding affinity of the receptor. Since the GABA binding sites are formed by the extracellular N-terminal domains, it was initially expected that the GABA EC_{50} of the chimeric subunits would be similar to the subunit that contributed this region or, alternatively, intermediate to the wild-type isoforms. Instead, receptors containing the α1/α6-A and -B site chimeras were *less* sensitive to GABA than either wild-type isoform (Fig. 4), with average EC_{50} values of $94.8 \pm 10.2\ \mu$M (α1/α6-A, $n = 5$) and $117.2 \pm 4.4\ \mu$M (α1/α6-B, $n = 6$) ($P > 0.2$ compared with one another, $P < 0.05$ compared with $\alpha1\beta3\gamma2$L). Conversely, receptors with the α6/α1-A or -B chimeric subunits were *more* sensitive to GABA than the wild-type receptors, with average EC_{50} values of $0.45 \pm 0.14\ \mu$M (α6/α1- A, $n = 4$) and $0.48 \pm 0.06\ \mu$M (α6/α1-B, $n = 6$) ($P > 0.2$ compared with one another, $P < 0.05$ compared with $\alpha6\beta3\gamma2$L). The GABA sensitivity of receptors containing the C-site chimeras was similar to the wild-type subunit that contributed their N-terminal structure, with average EC_{50} values of $19.1 \pm 2.9\ \mu$M (α1/α6-C, $n = 7$, $P > 0.2$ compared with $\alpha1\beta3\gamma2$L) and $1.7 \pm 0.3\ \mu$M (α6/α1-C, $n = 5$, $P > 0.2$ compared with $\alpha6\beta3\gamma2$L). These shifts in GABA sensitivity are consistent with a previous report examining only the A-site chimeric subunits (Fisher *et al.* 1997).

These results suggest that the regions between splice sites B and C influence GABA sensitivity for both the α1 and α6 subunits. This portion of the subunit includes TM3 and the TM3–TM4 intracellular loop. When this region is contributed from the α1 subunit, the EC_{50} is decreased, whereas when it is contributed from the α6 subunit, EC_{50} is increased. Structures in transmembrane or intracellular domains have not been suggested to form part of the agonist-binding pockets or directly alter GABA affinity. However, they could affect GABA EC_{50} by altering the signal transduction or gating transitions downstream of agonist binding (Colquhoun, 1998). The observed shifts in GABA sensitivity are consistent with the single channel properties conferred by the chimeric subunits. Channels with longer open time and burst duration should produce an apparent higher agonist affinity, even with no changes in the binding steps, if the agonist is less able to unbind from the open conformations. Conversely, simply reducing open time and burst duration can shift the equilibrium toward receptor conformations from which agonist unbinds, causing an apparent reduction in GABA sensitivity.

Effect of GABA concentration on receptor activation

Because of the potential influence of downstream gating transitions, concentration–response relationships and measurements of EC_{50} values often provide a poor estimate of agonist binding characteristics for ligand-gated channels (Colquhoun, 1998). The dependence of the channel activation rates on agonist concentration has been used to differentiate binding rates, or affinity, from the signal transduction processes that gate the channel, or efficacy (Clements & Westbrook, 1991; Lewis *et al.* 2003). The current rise time in response to agonist concentrations below EC_{50} values is related to binding affinity, while the maximum rise time, seen with saturating concentrations, is determined in large part by channel gating properties. The relationship between the activation rate and the GABA concentration was examined for receptors containing wild-type or chimeric subunits to clarify the structural determinants underlying the differences between the α1 and α6 subtypes in agonist binding and channel gating.

GABA concentrations from $1\ \mu$M to 10 mM were rapidly applied for 400 ms to excised outside-out patches held at -50 to -70 mV and the time for the current to increase from 10 to 90% of the peak response measured. At higher, saturating concentrations (1–10 mM), receptors containing the α1 subtype had rise times about 2 times faster than those containing the α6 subtype (Fig. 5*A*). This is consistent with greater gating efficacy for the $\alpha1\beta3\gamma2$L isoform. Increasing GABA concentration from 1 to 10 mM did not substantially alter the rise time, suggesting that the receptor binding sites are saturated by 1 mM GABA for both receptor isoforms. As anticipated from the higher GABA sensitivity of the $\alpha6\beta3\gamma2$L receptors, the rise times at GABA concentrations below $100\ \mu$M were significantly faster than those seen for the $\alpha1\beta3\gamma2$L receptors (Fig. 5*B*).

Receptors containing the chimeric subunits showed a mixed pattern of dependence on GABA concentration (Fig. 5*A* and *B*). The α1/α6-C and α6/α1-C chimeric subunits produced rise times similar to the wild-type subunit that contributed the N-terminal domain. Receptors with the α1/α6-A or α1/α6-B chimeric subunits had rise times like the $\alpha1\beta3\gamma2$L receptor at concentrations below $100\ \mu$M (Fig. 5*B*). Although the whole-cell concentration–response relationships indicated that these subunits reduced GABA sensitivity, the similarity in rise times at low GABA concentrations suggests that the binding rate was not different from the receptors containing the α1 subunit. At higher GABA concentrations, receptors containing the α1/α6-A or α1/α6-B chimeric subunits had rise times similar to $\alpha6\beta3\gamma2$L receptors, with maximum rates significantly slower than the $\alpha1\beta3\gamma2$L isoform (Fig. 5*A* and *B*). This is consistent with the channel gating properties of these receptors, which are similar to receptors containing the α6 subunit.

In a comparable pattern, receptors containing the α6/α1-A or α6/α1-B chimeric subunits had rise times like the $\alpha6\beta3\gamma2$L receptor at concentrations below $100\ \mu$M

(Fig. 5*B*). Again, the whole-cell studies showed that these subunits increased GABA sensitivity, but these results suggest that the binding affinity was not different from $\alpha6\beta3\gamma2$L receptors. At higher GABA concentrations, receptors containing these chimeric subunits had rise times similar to $\alpha1\beta3\gamma2$L receptors, with maximum rates significantly faster than the $\alpha6\beta3\gamma2$L isoform (Fig. 5*A* and *B*). This is consistent with higher gating efficacy, like that conferred by the $\alpha1$ subunit and as seen in the single channel recordings.

Desensitization of receptors containing $\alpha1$ or $\alpha6$ subunit subtypes

Most recombinant and native GABARs show desensitization, a decrease in current amplitude with continued agonist application. Entry into fast desensitized states can influence current rise times as well as deactivation rates following removal of agonist. The desensitization properties of receptors containing $\alpha1$ subunits have been well characterized, and depending upon the duration of application, are typically fitted with the sum of two to four exponential distributions (Haas & Macdonald, 1999). Conflicting findings have been reported for recombinant $\alpha6\beta$x$\gamma2$ receptors, with an early study showing little desensitization (Tia *et al.* 1996*b*) while more recent work found substantial fast desensitization (Bianchi *et al.* 2002).

When 1 mM GABA was applied for 400 ms, no significant differences were observed between the $\alpha1\beta3\gamma2$L and $\alpha6\beta3\gamma2$L receptor isoforms (Fig. 5*C*). The current decay during the application period was fitted with the sum of two exponential components for both isoforms. For receptors containing the $\alpha1$ subunit, the weighted average time constant for the current decay was 50.2 ± 11.2 ms. The two components had averages of 8.4 ± 0.9 ms ($63.6 \pm 3.8\%$) and 128.9 ± 31.8 ms, with an average residual current of $33.1 \pm 2.3\%$. The $\alpha6$ subunit-containing receptors showed similar characteristics, with averages of 10.9 ± 1.8 ms ($61.2 \pm 3.6\%$) and 128.9 ± 11.8 ms and a weighted average of 55.9 ± 5.8 ms. The average current remaining at the end of the application was $27.8 \pm 3.1\%$ of the peak current.

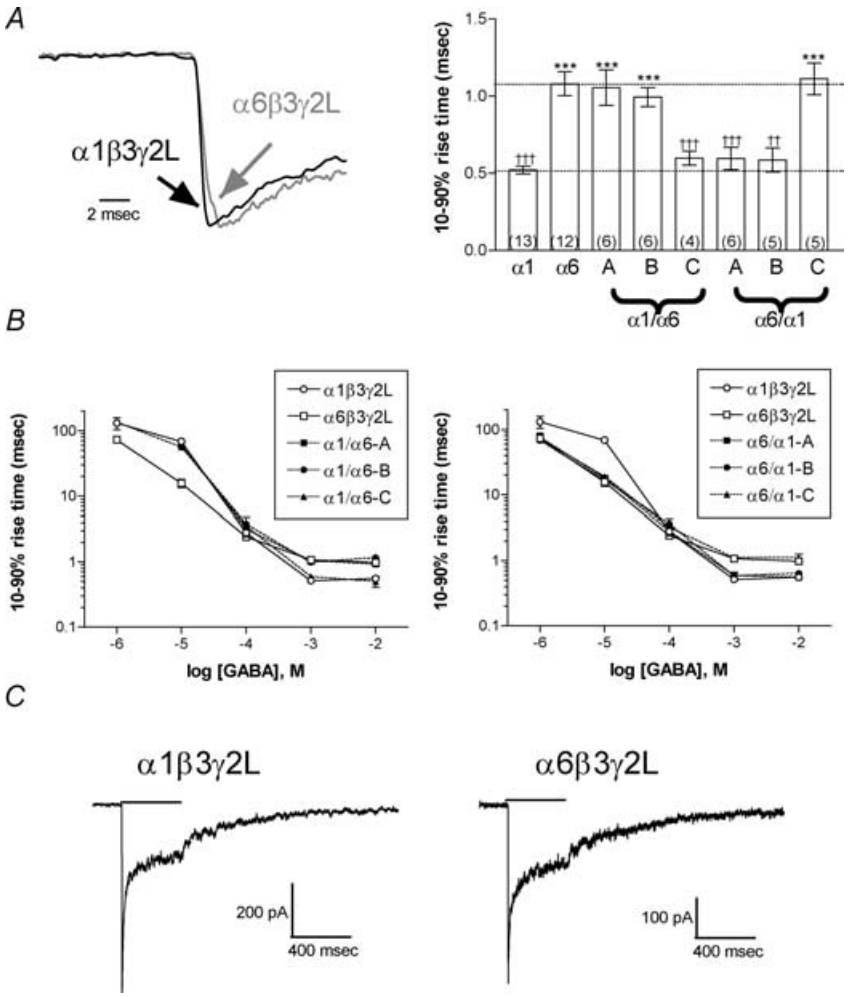

Figure 5. Rise time and desensitization properties
A, outside out macropatches were pulled from transfected cells and 1 mM GABA applied for 400 ms. Traces show current rise of $\alpha1\beta3\gamma2$L (black trace) and $\alpha6\beta3\gamma2$L (grey trace). Current amplitude was normalized to allow comparison of rise time. 1 mM GABA produced the maximum 10–90% rise time for receptor isoforms containing wild-type or chimeric subunits. Symbols and bars represent the average ± S.E.M. and the number in parentheses indicates number of patches. $^{**}P < 0.01$ and $^{***}P < 0.001$ indicate a significant difference from $\alpha1\beta3\gamma2$L while $\dagger\dagger P < 0.01$ and $\dagger\dagger\dagger P < 0.001$ indicate a significant difference from $\alpha6\beta3\gamma2$L. Dashed lines show the average response for the $\alpha1\beta3\gamma2$L and $\alpha6\beta3\gamma2$L isoforms. *B*, GABA concentrations ranging from 1 μM to 10 mM were applied for 400 ms to excised patches voltage clamped at −50 to −70 mV. Symbols and bars represent the average time ± S.E.M. for the current to increase from 10 to 90% of the maximal current ($n = 3$–13 patches). No data were obtained at 1 μM GABA for the $\alpha1/\alpha6$-A or $\alpha1/\alpha6$-B chimeric subunits because of low current amplitude. *C*, 1 mM GABA was applied for 400 ms to excised patches held at −50 to −70 mV to examine onset of desensitization. The current decay was fitted with the sum of two exponential components with similar kinetic properties for both $\alpha1\beta3\gamma2$L and $\alpha6\beta3\gamma2$L isoforms.

Deactivation kinetics of receptors containing wild-type and chimeric subunits

Differences in single channel kinetic properties and/or agonist binding affinity would be expected to alter the characteristics of the synaptic currents mediated by receptors containing the α1 or α6 subunits. Stable, agonist-bound conformations, such as long-duration open or closed (desensitized) states, serve to 'trap' the agonist in a high-affinity binding state (Bianchi & Macdonald, 2001). The previous results suggest that entry into fast desensitized states is similar for receptors containing either the α1 or α6 subtype. Therefore, in the absence of other effects, increasing open time and/or burst durations is predicted to slow deactivation in addition to decreasing GABA EC$_{50}$ (Colquhoun, 1998; Bianchi & Macdonald, 2001). To estimate the kinetic properties of postsynaptic currents, a saturating GABA concentration (1 mM) was applied for < 8 ms to outside-out macropatches held at -50 to -70 mV. The deactivation rate was determined for receptors containing either the wild-type α1 or α6 subunits or the chimeric subunits. Decay currents were fitted with the sum of two exponential distributions and weighted means were calculated by multiplying each time constant by its relative area.

The average decay time constant of the $\alpha6\beta3\gamma2$L receptors was significantly slower than that of the $\alpha1\beta3\gamma2$L receptors (Fig. 6). This is consistent with the higher GABA sensitivity (lower GABA EC$_{50}$) of the α6-containing receptor, but not with its single channel characteristics. A slower deactivation rate with incorporation of the α6 subunit compared with an α1 subunit was also observed with receptors containing the δ subunit (Bianchi *et al.* 2002). In that study, the properties of chimeric $\alpha1/\alpha6$ subunits suggested that the deactivation rate was determined primarily by structural differences within the extracellular N-terminal domain, possibly due to effects on ligand binding. Although no single channel kinetics were reported, the data suggested that a difference in binding affinity was the predominant determinant of the difference in deactivation.

Consistent with the relationship between GABA affinity and channel deactivation, the chimeric constructs with high sensitivity to GABA ($\alpha6/\alpha1$-A and -B) had the slowest deactivation rates while those with low sensitivity to GABA ($\alpha1/\alpha6$-A and -B), had very rapid deactivation rates (Fig. 6). The C-site chimeric subunits had deactivation time constants similar to the wild-type subunit that contributed their N-terminal domains.

The low gating efficacy (brief open time and burst durations) of the $\alpha6\beta3\gamma2$L channels would tend to speed deactivation. Therefore, it is most likely that its slower deactivation rate is due to a higher binding affinity for GABA and that this characteristic is associated with the extracellular N-terminal domain of the subunit. This is consistent with the concentration dependence of the current rise times. The even slower deactivation rates of the $\alpha6/\alpha1$-A and -B chimeric subunits would be predicted from their longer channel open time compared with the $\alpha6\beta3\gamma2$L receptor. These receptors would be expected to have high binding affinity similar to the α6 subunit (conferred by the N-terminal extracellular domain) and high efficacy gating (conferred by the TM3 and TM3–TM4 loop of the α1 subunit), both of which should slow deactivation. In contrast, receptors containing the $\alpha1/\alpha6$-A and -B chimeric subunits have shorter channel open times in addition to binding

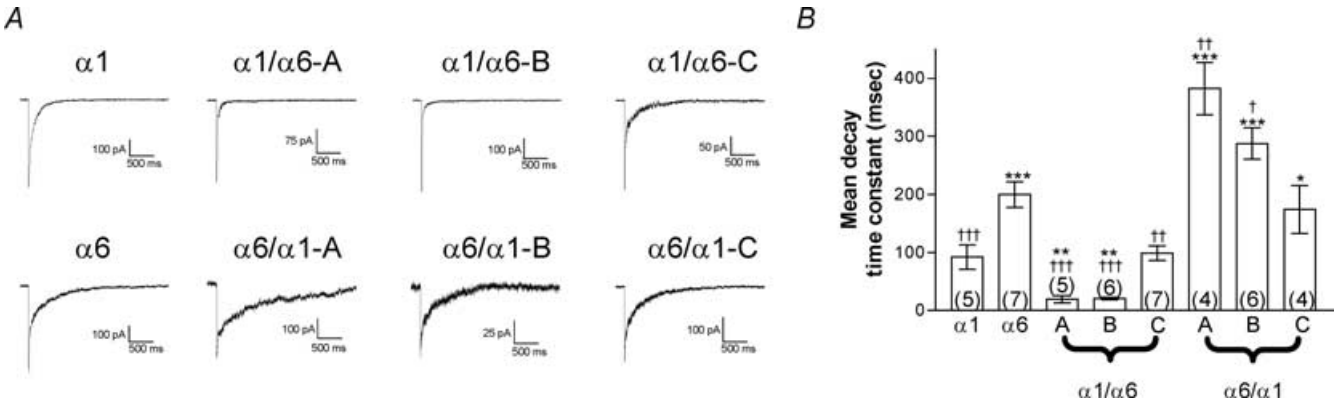

Figure 6. Current deactivation of receptors containing wild-type or chimeric subunits
A, outside out patches were pulled from cells transfected with the subunits indicated. GABA (1 mM) was applied for < 8 ms to cells voltage clamped at -50 to -70 mV. Traces shown are 3 s in duration. *B*, the current decay was fitted with the sum of 1–2 exponential components. Symbols and bars represent the weighted average ± S.E.M. and the number in parentheses indicates number of patches. $^*P < 0.05$, $^{**}P < 0.01$ and $^{***}P < 0.001$ indicate a significant difference from $\alpha1\beta3\gamma2$L while $\dagger P < 0.05$, $\dagger\dagger P < 0.01$ and $\dagger\dagger\dagger P < 0.001$ indicate a significant difference from $\alpha6\beta3\gamma2$L.

characteristics conferred by the N-terminal domain of the $\alpha 1$ subunit, leading to their very rapid deactivation rates.

Discussion

The GABAR $\alpha 1$ and $\alpha 6$ subunit subtypes have very different expression patterns in the mammalian brain and have been shown to confer distinct pharmacological and functional properties to recombinant and native receptors. These results show that these subtypes also produce channels with different single channel gating kinetics. Channel openings from the $\alpha 1\beta 3\gamma 2$L isoform were relatively long in duration, and were organized into multi-opening bursts. The $\alpha 6\beta 3\gamma 2$L isoform, in contrast, had brief-duration, isolated openings, suggesting that GABA acts as a low efficacy agonist at this receptor. While there are no previous reports of the single channel kinetic properties of receptors containing an $\alpha 6$ subunit, these findings are consistent with the single channel traces published for an allelic variant of $\alpha 6$ subunit shown in Angelotti *et al.* (1992), for which no kinetic analysis was reported. These characteristics are also similar to GABA-activated channels from recombinant $\alpha 4\beta 2\gamma 2$ receptors (Akk *et al.* 2004) as well as receptors containing the δ subunit (Fisher & Macdonald, 1997). The $\alpha 4$ and $\alpha 6$ subtypes are structurally related, and share many pharmacological characteristics. Therefore, it may not be surprising that they confer similar kinetic properties. Interestingly, it has been argued that GABA acts as a lower efficacy or partial agonist at δ subunit-containing receptors (Bianchi & Macdonald, 2003). Pentobarbital and some neurosteroids are more effective agonists than GABA at δ subunit-containing receptors, and single channel recordings have shown that they can produce long-duration openings and bursts, unlike GABA (Bianchi & Macdonald, 2003; Feng *et al.* 2004). These agonists also produce greater whole-cell current amplitudes than GABA at $\alpha 6\beta\gamma$ receptors (Thompson *et al.* 1996; Belelli *et al.* 2002). Examination of the effect of pentobarbital or neurosteroid agonists at the single channel level may confirm that receptors containing the $\alpha 6$ subunit are capable of producing long-duration openings in response to agonists that are more effective than GABA.

Alterations or abnormalities in $\alpha 1$ and $\alpha 6$ subunit expression may lead to the development of neurological and behavioural disorders. A shift from slow to fast decay kinetics has been correlated in several neurone populations to an increase in $\alpha 1$ subunit expression and a corresponding decrease in the $\alpha 2$ and $\alpha 3$ subunits (Brussaard *et al.* 1997; Robello *et al.* 1999; Okada *et al.* 2000; Hutcheon *et al.* 2000; Mellor *et al.* 2000; Vicini *et al.* 2001; Brussaard & Herbison, 2000; Bosman *et al.* 2002). The cerebellar localization of the $\alpha 6$ subunit suggests that it may be involved in motor control, particularly in the motor effects of ethanol and other sedatives (Korpi *et al.* 1993). Chronic treatment with benzodiazepines increases $\alpha 6$ subunit expression and decreases $\alpha 1$ subunit expression (O'Donovan *et al.* 1992). Since $\alpha 6$ subunit-containing receptors are insensitive to benzodiazepines, this change may lead to tolerance, a commonly observed clinical problem. A similar pattern of change is seen with alcohol dependence, as chronic ethanol administration increases $\alpha 6$ mRNA and decreases $\alpha 1$ mRNA (Mhatre & Ticku, 1992). Reducing the $\alpha 6$ subunit expression in cerebellar granule cells decreased agonist affinity, consistent with the higher GABA sensitivity of $\alpha 6$ subunit-containing recombinant receptors (Zhu *et al.* 1996; Makela *et al.* 1997). Extrasynaptic receptors containing the $\alpha 6$ subunit are believed to contribute the tonic current observed in cerebellar granule cells (Brickley *et al.* 1996; Rossi & Hamann, 1998; Nusser *et al.* 1998).

The properties of receptors containing $\alpha 1/\alpha 6$ chimeric subunits suggest that differences in GABA sensitivity and deactivation rate are predominately determined by the extracellular N-terminal domain. However, these characteristics are also influenced by channel gating properties, which appear to be conferred by the TM3 and/or the TM3–TM4 intracellular loop. We still lack a full understanding of physical changes in channel structure that underlie gating of the GABAR. Combined with studies of the structurally related glycine and nAChRs, hydrophobic residues within TM2 have been suggested to serve as the channel gate (Unwin, 2003). The conformational changes that result in channel opening may involve rotating or tilting of the TM2 helices (Tang *et al.* 2002; Unwin, 2003; Lester *et al.* 2004). Therefore it was somewhat surprising that the regions surrounding and including TM2 did not appear to be responsible for the kinetic differences associated with the $\alpha 1$ and $\alpha 6$ subtypes. Residues within this domain line the channel pore and are important for regulation of many channel properties, including gating, conductance and permeability and mediate the effects of some allosteric modulators (Karlin & Akabas, 1995; Mehta & Ticku, 1999). In addition, recent evidence has shown that electrostatic interactions between charged residues in the N-terminal and TM2–TM3 extracellular domains of the α subunits are important in signal transduction of agonist binding (Kash *et al.* 2003). However, the structure of the subunits in this region is highly conserved, with only five amino acids different between the $\alpha 1$ and $\alpha 6$ subtypes from splice site A to B. While this domain may be important for many general GABAR channel properties, structural differences within it do not appear responsible for the distinct single channel properties associated with the $\alpha 1$ and $\alpha 6$ subtypes.

The possibility that the structures within TM3 may control gating characteristics is interesting. Electron

microscopy suggests that this domain interacts with the TM2 domain, possibly regulating its movement during activation (Miyazawa *et al.* 2003). The TM2 and TM3 domains have been suggested to contribute to a water-filled cavity, which forms the binding pocket for volatile anaesthetics and ethanol (Mihic *et al.* 1997; Krasowski *et al.* 1998, 2001; Ueno *et al.* 1999; Krasowski & Harrison, 2000). It has been reported that several residues within TM3 are accessible to the aqueous solution, and that changes in its secondary structure occur with GABA binding (Williams & Akabas, 1999). Recent studies examining cross-linking of engineered cysteine residues also provided evidence for a close relationship between residues within TM2 and TM3 of the glycine receptor subunits (Lobo *et al.* 2004). The TM3 domain is highly conserved among the GABAR subunits, and there are only two residues that differ between the α1 and α6 subtypes. Mutations of residues within TM3 increase spontaneous activity of the GABAR (Ueno *et al.* 1999) and have been shown to affect gating kinetics of the nAChR (Campos-Caro *et al.* 1997; Wang *et al.* 1999). Recently, an inherited form of epilepsy was reported in which the alanine 294 residue within the TM3 of the α1 subunit is mutated to aspartate (Cossette *et al.* 2002). Kinetic analysis of recombinant receptors showed that the mutation accelerated deactivation, slowed desensitization and reduced channel open time, consistent with a role for the TM3 in regulating channel gating efficacy (Fisher, 2004).

Regulation of GABAR kinetic properties by structures within the TM3–TM4 intracellular loop is also a strong possibility, especially as this region exhibits substantial heterogeneity among subunit subtypes. Since phosphorylation of residues within the intracellular loop of several subunits alters receptor function, structural changes within this domain are clearly able to influence channel behaviour (Mehta & Ticku, 1999). Genetic studies have linked a mutation (P385S) in this domain of the human α6 subunit to alcoholism and reduced sensitivity to the motor and anxiolytic effects of benzodiazepine agonists (Iwata *et al.* 1999, 2000; Hoffman *et al.* 2002). In structurally related receptors, a mutation that encoded a six amino acid duplication within the intracellular loop of the nAChR altered its gating kinetics (Milone *et al.* 1998) while this region of the 5HT$_3$ serotonin receptor was found to influence its single channel conductance (Kelley *et al.* 2003). Interactions between the M3–M4 intracellular domain and M4 have been proposed to control channel gating of the nAChR (Akk & Steinbach, 2000).

Further studies examining the role of individual residues within these domains of the α subunit subtypes as well as other GABAR subunit family members may shed more light on the structures that regulate the kinetic properties of ligand-gated channels.

References

Akk G, Bracamontes J & Steinbach JH (2004). Activation of GABA$_A$ receptors containing the α4 subunit by GABA and pentobarbital. *J Physiol* **566**, 387–399.

Akk G & Steinbach JH (2000). Structural elements near the C-terminus are responsible for changes in nicotinic gating kinetics following patch excision. *J Physiol* **527**, 405–417.

Angelotti TP & Macdonald RL (1993). Assembly of GABA$_A$ receptor subunits: $\alpha1\beta1$ and $\alpha1\beta1\gamma2$S subunits produce unique ion channels with dissimilar single-channel properties. *J Neurosci* **13**, 1429–1440.

Angelotti TP, Tan F, Chahine KG & Macdonald RL (1992). Molecular and electrophysiological characterization of a allelic variant of the rat α6 GABA$_A$ receptor subunit. *Mol Brain Res* **16**, 173–178.

Angelotti TP, Uhler MD & Macdonald RL (1993). Assembly of GABA$_A$ receptor subunits: analysis of transient single-cell expression utilizing a fluorescent substrate/marker gene technique. *J Neurosci* **13**, 1418–1428.

Belelli D, Casula A, Ling A & Lambert JJ (2002). The influence of subunit composition on the interaction of neurosteroids with GABA$_A$ receptors. *Neuropharm* **43**, 651–661.

Bianchi MT, Haas KF & Macdonald RL (2002). α1 and α6 subunits specify distinct desensitization, deactivation and neurosteroid modulation of GABA$_A$ receptors containing the δ subunit. *Neuropharmacology* **43**, 492–502.

Bianchi MT & Macdonald RL (2001). Agonist trapping by GABA$_A$ receptor channels. *J Neurosci* **21**, 9083–9091.

Bianchi MT & Macdonald RL (2003). Neurosteroids shift partial agonist activation of GABA$_A$ receptor channels from low- to high-efficacy gating patterns. *J Neurosci* **23**, 10934–10943.

Bosman LWJ, Rosahl TW & Brussaard AB (2002). Neonatal development of the rat visual cortex: synaptic function of GABA$_A$ receptor α subunits. *J Physiol* **545**, 169–181.

Brickley SG, Cull-2 SG & Farrant M (1996). Development of a tonic form of synaptic inhibition in rat cerebellar granule cells resulting from persistent activation of GABA$_A$ receptors. *J Physiol* **497**, 753–759.

Brussaard AB & Herbison AE (2000). Long-term plasticity of postsynaptic GABA$_A$-receptor function in the adult brain: insights from the oxytocin neurone. *Trends Neurosci* **23**, 190–195.

Brussaard AB, Kits KS, Baker RE, Willems WPA, Leyting-Vermeulen JW, Voorn P, Smit AB, Bicknell RJ & Herbison AE (1997). Plasticity in fast synaptic inhibition of adult oxytocin neurons caused by switch in GABA$_A$ receptor subunit expression. *Neuron* **19**, 1103–1114.

Burgard EC, Tietz EI, Neelands TR & Macdonald RL (1996). Properties of recombinant γ-aminobutyric acid$_A$ receptor isoforms containing the α5 subunit subtype. *Mol Pharm* **50**, 119–127.

Cagetti E, Liang J, Spigelman I & Olsen RW (2003). Withdrawal from chronic intermittent ethanol treatment changes subunit composition, reduces synaptic function, and decreases behavioral responses to positive allosteric modulators of GABA$_A$ receptors. *Mol Pharm* **63**, 53–64.

Campos-Caco A, Rovira JC, Vicente-Agullo F, Ballesta JJ, Sala S, Criado M & Sala F (1997). Role of the putative transmembrane segment M3 in gating of neuronal nicotinic receptors. *Biochemistry* **36**, 2709–2715.

Chesnut JD, Baytan AR, Russell M, Chang MP, Bernard A, Maxwell IH & Hoeffler JP (1996). Selective isolation of transiently transfected cells from a mammalian cell population with vectors expressing a membrane anchored single-chain antibody. *J Immunol Meth* **193**, 17–27.

Clements JD & Westbrook GL (1991). Activation kinetics reveal the number of glutamate and glycine binding sites on the N-methyl-D-aspartate receptor. *Neuron* **7**, 605–613.

Colquhoun D (1998). Binding, gating, affinity and efficacy: the interpretation of structure-activity relationships for agonists and of the effects of mutating receptors. *Br J Pharm* **125**, 924–947.

Colquhoun D & Sakmann B (1985). Fast events in single-channel currents activated by acetylcholine and its analogues at the frog muscle end-plate. *J Physiol* **369**, 501–557.

Colquhoun D & Sigworth FJ (1995). Fitting and statistical analysis of single-channel records. In *Single-Channel Recording*, ed. Sackmann B & Neher E, 2nd edn, pp. 483–587. Plenum Press, New York.

Cossette P, Liu L, Brisebois K, Dong H, Lortie A, Vanasse M, Saint-Hilaire J-M, Carmant L, Verner A, Lu W-Y, Wang YT & Rouleau GA (2002). Mutation of GABRA1 in an autosomal dominant form of juvenile myoclonic epilepsy. *Nature Genet* **31**, 184–189.

Ducic I, Caruncho HJ, Zhu WJ, Vicini S & Costa E (1995). γ-aminobutyric acid gating of Cl^- channels in recombinant $GABA_A$ receptors. *J Pharmacol Exp Ther* **272**, 438–445.

Feng HJ, Bianchi MT & Macdonald RL (2004). Pentobarbital differentially modulates $\alpha1\beta3\delta$ and $\alpha1\beta3\gamma2$L $GABA_A$ receptor currents. *Mol Pharmacol* **66**, 981–1003.

Fisher JL (2004). A mutation in the $GABA_A$ receptor $\alpha1$ subunit linked to human epilepsy affects channel gating properties. *Neuropharm* **46**, 629–637.

Fisher JL & Macdonald RL (1997). Single-channel properties of $GABA_A$ receptors containing $\gamma2$ or δ subtypes expressed with $\alpha1$ and $\beta3$ subtypes in L929 cells. *J Physiol* **505**, 283–297.

Fisher JL, Zhang J & Macdonald RL (1997). The role of $\alpha1$ and $\alpha6$ subtype amino-terminal domains in allosteric regulation of γ-aminobutyric $acid_a$ receptors. *Mol Pharmacol* **52**, 714–724.

Gingrich KJ, Roberts WA & Kass RS (1995). Dependence of the $GABA_A$ receptor gating kinetics on the α-subunit isoform: implications for structure–function relations and synaptic transmission. *J Physiol* **489**, 529–543.

Goldstein PA, Elsen FP, Ying S-W, Ferguson C, Homanics GE & Harrison NL (2002). Prolongation of hippocampal miniature inhibitory postsynaptic currents in mice lacking the $GABA_A$ receptor $\alpha1$ subunit. *J Neurophysiol* **88**, 3208–3217.

Greenfield LJ Jr, Sun F, Neelands TR, Burgard EC, Donnelly JL & Macdonald RL (1997). Expression of functional $GABA_A$ receptors in transfected L929 cells isolated by immunomagnetic bead separation. *Neuropharmacology* **36**, 63–73.

Haas KF & Macdonald RL (1999). $GABA_A$ receptor subunit $\gamma2$ and δ subtypes confer unique kinetic properties on recombinant $GABA_A$ receptor currents in mouse fibroblasts. *J Physiol* **514**, 27–45.

Hoffman WE, Balyasnikova IV, Mahay H, Danilov SM & Baughman VL (2002). GABA $\alpha6$ receptors mediate midazolam-induced anxiolysis. *J Clin Anesth* **14**, 206–209.

Horn R (1987). Statistical methods for model discrimination: applications to gating kinetics and permeation of the acetylcholine receptor channel. *Biophys J* **51**, 255–263.

Hsu F-C, Waldeck R, Faber DS & Smith SS (2003). Neurosteroid effects on GABAergic synaptic plasticity in hippocampus. *J Neurophys* **89**, 1929–1940.

Hutcheon B, Morley P & Poulter MO (2000). Developmental change in $GABA_A$ receptor desensitization kinetics and its role in synapse function in rat cortical neurons. *J Physiol* **522**, 3–17.

Iwata N, Cowley DS, Radel M, Roy-Byrne PP & Goldman D (1999). Relationship between a $GABA_A$ $\alpha6$ Pro385Ser substitution and benzodiazepine sensitivity. *Am J Psych* **156**, 1447–1449.

Iwata N, Virkkunen M & Goldman D (2000). Identification of a naturally occurring Pro385-Ser385 substitution in the $GABA_A$ receptor $\alpha6$ subunit gene in alcoholics and healthy volunteers. *Mol Psych* **5**, 316–319.

Karlin A & Akabas MH (1995). Toward a structural basis for the function of the nicotinic acetylcholine receptors and their cousins. *Neuron* **15**, 1231–1244.

Kash TL, Jenkins A, Kelley JC, Trudell JR & Harrison NL (2003). Coupling of agonist binding to channel gating in the $GABA_A$ receptor. *Nature* **421**, 272–275.

Kelley SP, Dunlop JI, Kirkness EF, Lambert JJ & Peters JA (2003). A cytoplasmic region determines single-channel conductance in 5-HT3 receptors. *Nature* **424**, 321–324.

Koksma J-J, van Kesteren RE, Rosahl TW, Swart R, Smit AB, Lüddens H & Brussaard AB (2003). Oxytocin regulates neurosteroid modulation of $GABA_A$ receptors in supraoptic nucleus around parturition. *J Neurosci* **23**, 788–797.

Korpi ER, Gründer G & Lüddens H (2002). Drug interactions at $GABA_A$ receptors. *Prog Neurobiol* **67**, 113–159.

Korpi ER, Kleingoor C, Kettenmann H & Seeburg PH (1993). Benzodiazepine-induced motor impairment linked to point mutation in cerebellar $GABA_A$ receptor. *Nature* **361**, 356–359.

Krasowski MD & Harrison NL (2000). The actions of ether, alcohol and alkane general anaesthetics on $GABA_A$ and glycine receptors and the effects of TM2 and TM3 mutations. *Br J Pharm* **129**, 731–743.

Krasowski MD, Koltchine VV, Rick CE, Ye Q, Finn SE & Harrison NL (1998). Propofol and other intravenous anesthetics have sites of action on the γ-aminobutyric acid type A receptor distinct from that for isoflurane. *Mol Pharmacol* **53**, 530–538.

Krasowski MD, Nishikawa K, Nikolaeva N, Lin A & Harrison NL (2001). Methionine 286 in transmembrane domain 3 of the $GABA_A$ receptor β subunit controls a binding cavity for propofol and other alkylphenol general anesthetics. *Neuropharm* **41**, 952–964.

Laurie DJ, Seeburg PH & Wisden W (1992*b*). The distribution of 13 $GABA_A$ receptor subunit mRNAs in the rat brain. III. Olfactory bulb and cerebellum. *J Neurosci* **12**, 1063–1076.

Laurie DJ, Wisden W & Seeburg PH (1992*a*). The distribution of thirteen $GABA_A$ receptor subunit mRNAs in the rat brain. III. Embryonic and postnatal development. *J Neurosci* **12**, 4151–4172.

Lavoie AM, Tingey JJ, Harrison NL, Pritchett DB & Twyman RE (1997). Activation and deactivation rates of recombinant $GABA_A$ receptor channels are dependent on α-subunit isoform. *Biophys J* **73**, 2518–2526.

Lester HA, Dibas MI, Dahan DS, Leite JF & Dougherty DA (2004). Cys-loop receptors: new twists and turns. *Trends Neurosci* **27**, 329–336.

Lewis TM, Schofield PR & McClellan AML (2003). Kinetic determinants of agonist action at the recombinant human glycine receptor. *J Physiol* **549**, 361–374.

Lobo IA, Trudell JR & Harris RA (2004). Cross-linking of glycine receptor transmembrane segments two and three alters coupling of ligand binding with channel opening. *J Neurochem* **90**, 962–969.

Lüddens H, Pritchett DB, Köhler M, Killisch I, Keinänen Monyer H, Sprengel R & Seeburg PH (1990). Cerebellar $GABA_A$ receptor selective for a behavioural alcohol antagonist. *Nature* **346**, 648–651.

McClellan AML & Twyman RE (1999). Receptor system response kinetics reveal functional subtypes of native murine and recombinant human $GABA_A$ receptors. *J Physiol* **515**, 711–727.

McKernan RM & Whiting PJ (1996). Which $GABA_A$-receptor subtypes really occur in the brain? *Trends Neurosci* **19**, 139–143.

Makela R, Uusi-Oukari M, Homanics GE, Quinlan JJ, Firestone LL, Wisden W & Korpi ER (1997). Cerebellar γ-aminobutyric acid type A receptors: pharmacological subtypes revealed by mutant mouse lines. *Mol Pharm* **52**, 380–388.

Mehta AK & Ticku MK (1999). An update on $GABA_A$ receptors. *Brain Res Rev* **29**, 196–217.

Mellor JR, Wisden W & Randall AD (2000). Somato-synaptic variation of $GABA_A$ receptors in cultured murine cerebellar granule cells: investigation of the role of the α6 subunit. *Neuropharm* **39**, 1495–1513.

Mhatre MC & Ticku MK (1992). Chronic ethanol administration alters γ-aminobutyric $acid_A$ receptor gene expression. *Mol Pharmacol* **42**, 415–422.

Mihic SJ, Ye Q, Wick MJ, Koltchine VV, Krasowski MD, Finn SE, Mascia MP, Valenzuela CF, Hanson KK, Greenblatt EP, Harris RA & Harrison NL (1997). Sites of alcohol and volatile anaesthetic action on $GABA_A$ and glycine receptors. *Nature* **389**, 385–389.

Milone M, Wang H-L, Ohno K, Prince R, Fukudome T, Schen X-M, Brengman JM, Griggs RC, Sine SM & Engel AG (1998). Mode switching kinetics produced by a naturally occurring mutation in the cytoplasmic loop of the human acetylcholine receptor ε subunit. *Neuron* **20**, 575–588.

Miyazawa A, Fujiyoshi Y & Unwin N (2003). Structure and gating mechanism of the acetylcholine receptor pore. *Nature* **423**, 949–955.

Nusser Z, Sieghart W & Somogyi P (1998). Segregation of different $GABA_A$ receptors to synaptic and extrasynaptic membranes of cerebellar granule cells. *J Neurosci* **18**, 1693–1703.

O'Donovan MC, Buckland PR, Spurlock G & McGuffin P (1992). Bidirectional changes in the levels of messenger RNA encoding γ-aminobutyric $acid_A$ receptor α subunits after flurazepam treatment. *Eur J Pharm* **226**, 335–341.

Okada M, Onodera K, Van Renterghem C, Sieghart W & Takahashi T (2000). Functional correlation of $GABA_A$ receptor α subunits expression with the properties of IPSCs in the developing thalamus. *J Neurosci* **20**, 2202–2208.

Robello M, Amico C & Cupello A (1999). Evidence of two populations of $GABA_A$ receptors in cerebellar granule cells in culture: different desensitization kinetics, pharmacology, serine/threonine kinase sensitivity, and localization. *Biochem Biophys Res Comm* **266**, 603–608.

Rossi DJ & Hamann M (1998). Spillover-mediated transmission at inhibitory synapses promoted by high affinity α6 subunit $GABA_A$ receptors and glomerular geometry. *Neuron* **20**, 783–795.

Saxena NC & Macdonald RL (1996). Properties of putative cerebellar γ-aminobutyric $acid_A$ receptor isoforms. *Mol Pharmacol* **49**, 567–579.

Smith SS, Gong QH, Li X, Moran MH, Bitran D, Frye CA & Hsu F-C (1998). Withdrawal from 3α-OH-5α-pregnan-20-one using a pseudopregnancy model alters the kinetics of hippocampal $GABA_A$-gated current and increases the $GABA_A$ receptor α4 subunit in association with increased anxiety. *J Neurosci* **18**, 5275–5284.

Tang P, Mandal PK & Xu Y (2002). NMR structures of the second transmembrane domain of the human glycine receptor α1 subunit: model of pore architecture and channel gating. *Biophys J* **83**, 252–262.

Thompson SA, Whiting PJ & Wafford KA (1996). Barbiturate interactions at the human $GABA_A$ receptor: dependence on receptor subunit combination. *Br J Pharm* **117**, 521–527.

Tia S, Wang JF, Kotchabhakdi N & Vicini S (1996*a*). Developmental changes of inhibitory synaptic currents in cerebellar granule neurons: role of $GABA_A$ receptor α6 subunit. *J Neurosci* **16**, 3630–3640.

Tia S, Wang JF, Kotchabhakdi N & Vicini S (1996*b*). Distinct deactivation and desensitization kinetics of recombinant $GABA_A$ receptors. *Neuropharm* **35**, 1375–1382.

Twyman RE, Rogers CJ & Macdonald RL (1990). Intra-burst kinetic properties of the $GABA_A$ receptor main conductance state of mouse spinal cord neurones in culture. *J Physiol* **423**, 193–220.

Tyndale RF, Olsen RW & Tobin AJ (1995). $GABA_A$ receptors. In *Ligand- and Voltage-Gated Ion Channels*, ed. North RA, pp. 265–290. CRC Press, Boca Raton.

Ueno S, Wick MJ, Ye Q, Harrison NL & Harris RA (1999). Subunit mutations affect ethanol actions on $GABA_A$ receptors expressed in *Xenopus* oocytes. *Br J Pharmacol* **127**, 377–382.

Unwin N (2003). Structure and action of the nicotinic acetylcholine receptor explored by electron microscopy. *FEBS Lett* **555**, 91–95.

Varecka L, Wu CH, Rotter A & Frostholm A (1994). $GABA_A$/benzodiazepine receptor α6 subunit mRNA in granule cells of the cerebellar cortex and cochlear nuclei: expression in developing and mutant mice. *J Comp Neurol* **339**, 341–352.

Vicini S, Ferguson C, Prybylowski K, Kralic J, Morrow AL & Homanics GE (2001). $GABA_A$ receptor $\alpha 1$ subunit deletion prevents developmental changes of inhibitory synaptic currents in cerebellar neurons. *J Neurosci* **21**, 3009–3016.

Wang HL, Ohno K, Milone M, Brengman J, Evoli A, Batocchi AP, Middleton LT, Christodoulou K, Engel AG & Sine SM (1999). Acetylcholine receptor M3 domain: stereochemical and volume contributions to channel gating. *Nat Neurosci* **2**, 226–233.

Williams DB & Akabas MH (1999). γ-aminobutyric acid increases the water accessibility of M3 membrane spanning segment residues in γ-aminobutyric acid type A receptors. *Biophys J* **77**, 2563–2574.

Zhu WJ, Wang JF, Vicini S & Grayson DR (1996). $\alpha 6$ and $\gamma 2$ subunit antisense oligonucleotides alter γ-amino butyric acid receptor pharmacology in cerebellar granule neurons. *Mol Pharmacol* **50**, 23–33.

Acknowledgements

Thanks to Annette Smith and Dr Steve Wilson for help with construction of the chimeric subunits and to Dr Paul Housley for preparation of the antigen-coated magnetic beads. This work was supported by the University of South Carolina School of Medicine Research Development Fund, the South Carolina Commission on Higher Education, the PhRMA foundation, the National Science Foundation/EPSCoR (EPS-1032573) and NIH/BRIN (8-P0RR16461A).